Modern Advances in Wireless Power Transfer Systems for Roadway Powered Electric Vehicles

Chunting Chris Mi, *Fellow, IEEE*, Giuseppe Buja, *Life Fellow, IEEE*, Su Y. Choi, *Member, IEEE*, and Chun T. Rim, *Senior Member, IEEE*

***Abstract*—Wireless power transfer system (WPTS)-based wireless electric vehicles, classified into roadway-powered electric vehicles (RPEVs) and stationary charging electric vehicles (SCEVs), are in the spotlight as future mainstream transportations. RPEVs are free from serious battery problems such as large, heavy, and expensive battery packs and long charging time because they get power directly from the road while moving. The power transfer capacity, efficiency, lateral tolerance, electromagnetic field, air-gap, size, weight, and cost of the WPTSs have been improved by virtues of innovative semiconductor switches, better coil designs, roadway construction techniques, and higher operating frequency. Recent advances in WPTSs for RPEVs are summarized in this review paper. The fifth- and sixth-generation online electric vehicles, which reduce infrastructure cost for commercialization, and the interoperability between RPEVs and SCEVs are addressed in detail in this paper. Major milestones of the developments of other RPEVs are also summarized. The rest of this paper deals with a few important technical issues such as coil structures, power supply schemes, and segmentation switching techniques of a lumped inductive power transfer system for RPEVs.**

***Index Terms*—Roadway powered electric vehicle (RPEV), wireless electric vehicle (WEV).**

I. Introduction

Wireless electric vehicles (WEVs) using wireless power transfer systems (WPTSs), which are classified into roadway powered electric vehicles (RPEVs), also referred to as dynamic charging electric vehicles, and stationary charging electric vehicles (SCEVs), have recently been in the spotlight as attractive alternatives to internal combustion vehicles. Pure battery EVs (PEVs), hybrid EVs (HEVs), plug-in hybrid EVs (PHEVs), and battery replace EVs are also proposed. Among them, the charging of PEVs and PHEVs has gradually changed from wired type to wireless type, which is the background of actively studied SCEVs.

Generally, WPTSs for WEVs can be divided into inductive power transfer systems (IPTSs) [1]–[64], coupled magnetic resonance systems (CMRSs) [65]–[67], and capacitive power transfer systems (CPTSs) [68]. It seems that these three WPTSs are totally different from each other; however, CMRSs are found to be just a special form of IPTSs having an extremely high quality factor (Q) [67]; also, it has been verified that 5-m-long-distance wireless power transfer can be effectively achieved with IPTSs using optimally shaped two dipole coils [97] instead of multiple CMRS coils. Moreover, the CMRSs not only have difficulty in maintaining resonance conditions due to their extremely high Q but are also too bulky to be installed at the bottom of a vehicle. For these reasons, CMRSs are far from the right candidate for WEVs [69]. Therefore, IPTSs have been considered as the most appropriate WPTS and are commonly used for RPEVs because they are not constrained from the aforementioned problems of CPTS and CMRS [69]. Among WEVs, RPEVs are becoming the most promising candidate for future transportation because they are ideally free from large, heavy, and expensive batteries, and get power directly while moving on a road. For more than its 100-year history, significant improvements of IPTSs for RPEVs in their power transfer capacity, efficiency, lateral and longitudinal tolerances, electromagnetic field (EMF), air-gap, size, weight, and cost have been achieved by virtues of innovative semiconductor power switches, coil designs, roadway construction techniques, and higher operating frequencies. Despite the fact that RPEVs are free from battery problems, RPEVs have not been widely used so far due to high initial investment cost for commercialization. To cope with this problem, in addition to new RPEV technology to effectively reduce the cost, strong motivation to build national infrastructures for RPEVs with public consent is needed. So the best deployment scenario would be that SCEVs are completely compatible with the IPTSs built for RPEVs. SCEVs will be widely deployed in the near future to replace the wired EV chargers of PHEVs and PEVs due to the convenience and safe operation of SCEVs. As a result of the growing interest in SCEVs, in 2010, the society of automotive engineers (SAE) established the SAE J2954 wireless charging task force to set the comprehensive standards for SCEVs such as transmitter and receiver coils, a feasible operating frequency band, air-gaps, power transfer levels and efficiencies, control strategies, foreign metal and living object detections, communication protocols, and magnetic and electric field regulations [70]. The standards are planned to be published in 2016,

Manuscript received November 9, 2015; revised February 3, 2016; accepted March 3, 2016. Date of publication June 14, 2016; date of current version September 9, 2016. This work was supported in part by the Samsung Research Funding Center of Samsung Electronics under Project SRFC-IT1301-06, in part by the KUSTAR-KAIST Institute, Korea Advanced Institute of Science and Technology (KAIST), and in part by the Ministry of Science, ICT & Future Planning, South Korea.

C. C. Mi is with the Department of Electrical and Computer Engineering, San Diego State University, San Diego, CA 92182 USA (e-mail: mi3032@gmail.com).

G. Buja is with the Department of Industrial Engineering, University of Padova, 35131 Padova, Italy (e-mail: giuseppe.buja@unipd.it).

S. Y. Choi and C. T. Rim are with the Department of Nuclear and Quantum Engineering, Korea Advanced Institute of Science and Technology, Daejeon 34141, South Korea (e-mail: suchoi@kaist.ac.kr; ctrim@kaist.ac.kr).

Color versions of one or more of the figures in this paper are available online at http://ieeexplore.ieee.org.

Digital Object Identifier 10.1109/TIE.2016.2574993

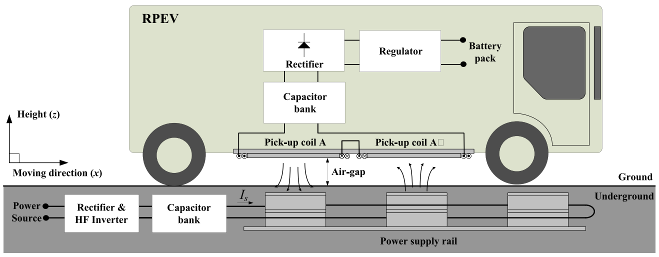

Fig. 1. Configuration of the IPTS for an RPEV.

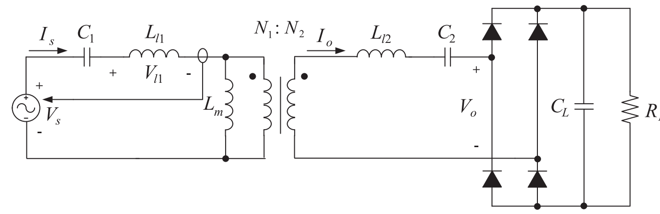

Fig. 2. Equivalent circuit of the current source series–series compensation (I-SS) scheme for an IPTS for RPEVs.

and it would be, therefore, worthwhile for us to follow up the SAE J2954 standard and design the IPTSs for RPEVs in accordance with the SAE J2954 for the interoperability between RPEVs and SCEVs.

As a follow-up to the previous review paper that dealt with a full history of WPTSs for RPEVs from their advent in the 1890s and important design considerations [69], recent studies of the past couple of years are newly summarized in this review paper. Above all, important technical issues in the new developments of the fifth- (5G) and sixth-generation (6G) online electric vehicles (OLEVs), which highly focus on the reduction of initial investment costs for commercialization as well as the interoperability between RPEVs and SCEVs, are addressed, while major milestones of the developments of other RPEVs are newly summarized. In the rest of this paper, some important technical issues, such as coil structures, power supply schemes, and segmentation switching techniques of a lumped IPTS for RPEVs have been addressed.

II. Fundamentals of RPEVs

A. Overall Configuration of RPEVs

As mentioned in the introduction section, most of the recent research teams for RPEVs adopt IPTSs for wireless power transfer purposes due to their highly efficient and robust power transfer characteristics to lateral displacements as well as relatively small transmitter and receiver coils compared to CMRSs and CPTSs. In general, the IPTS consists two subsystems [69]: one is the roadway subsystem to transfer power, which includes an HF inverter, a primary capacitor bank, and a power supply rail (or transmitter). The other one is the on-board subsystem to receive power from the roadway subsystem, and this includes a pick-up coil (or receiver), a secondary capacitor bank, a rectifier, and a regulator for a battery pack, as shown in Fig. 1.

B. Fundamental Principles of the IPTS

The IPTSs are basically governed by Ampere's and Faraday's laws among four Maxwell equations. The time-varying magnetic flux is generated from the ac current and unwanted leakage magnetic flux exposed to pedestrians and other electronic systems should be effectively mitigated to meet the ICNIRP guidelines [71], [72] and EMC tests for commercialization. For the EMF issue, therefore, there have been two main techniques: one is power rail segmentation techniques dividing a long power rail into multiple short power rails to selectively turn on power rails when RPEVs are on the power rails [69]. The other one is EMF cancellation techniques, which are divided into two methods: one is passive EMF cancel methods using 1) high-conductivity materials to cancel the unwanted magnetic flux by using induced eddy-current on the material surface or using 2) high-relative-permeability materials to guide the unwanted magnetic flux to the intended directions by providing a low magnetic reluctance path. The other one is active EMF cancellation methods [73]–[82], which include several complex systems such as additional coils, power sources, phasor detectors, and controllers to generate the opposite magnetic flux to cancel the unwanted magnetic flux. In addition, compensation circuits are necessary for an IPTS of RPEVs to maximize its output power. It is critical to select an appropriate compensation circuit at the beginning of IPTS designs, considering critical electrical characteristics such as maximum efficiency conditions, maximum load power transfer conditions, load-independent output power conditions, coupling coefficient independent compensation conditions, and allowance for the absence of RPEVs. Among many compensation schemes, the current source series–series compensation scheme, as shown in Fig. 2, as well as the current source series–parallel compensation scheme, are viable solutions to meet all the mentioned electrical characteristics [83].

C. The Early History of RPEV

The origin of the RPEV is found in the U.S. patent of the transformer system for electric railways by Hutin and Leblanc in France in 1894 [1], and the basic configuration of this transformer system is almost the same as modern IPTSs. Moreover, several important design features of IPTSs for RPEVs, such as the deployment of power supply rails, compensation schemes, high-power transfer to pick-up coils, and reduction of conduction and eddy current losses, have been claimed in the patent. About 100 year later, as a result of the growing interest in RPEVs due to the oil crisis in the 1970s, three projects were undertaken in the U.S. to investigate RPEVs in order to minimize the petroleum use of vehicles [2]–[9]. The first project was started in 1976 by the Lawrence Berkeley National Laboratory while the Santa Barbara Electric Bus Project was started in 1979. During these two projects, several prototype RPEVs were developed but not appropriately operated. After the previous two projects of RPEVs, the University of California, Berkeley, undertook the Partners for Advanced Transit and Highways (PATH) program in 1992 to validate the technical viability of RPEVs. Through the PATH program, broad investigation and field tests on RPEVs were performed and the PATH team developed the first RPEV buses, which achieved an efficiency of 60% at an output power of 60 kW with a 7.6 cm air-gap [69]. The RPEV buses, however, had not been commercialized because they used a low operating frequency of 400 Hz due to the absence of fast power switches, good ferrite cores, and litz wires. As a result, a high-power rail construction cost of around 1 M$/km, a large power rail current of thousands amperes, a heavy power supply and pick-up coils, acoustic noises, and low system efficiencies were obtained. In addition, the small air-gap, lateral tolerance, and large EMF level are not acceptable for its commercialization.

III. Developments of OLEVs

Since 2009, the OLEV project has been conducted by a research team led by KAIST [10]–[43], and this project has solved most of the remaining problems of the PATH project for commercialization such as high-frequency current-controlled inverters, continuous power transfers, low EMF characteristics [10]–[16], [18]–[20], dynamic response analysis for high-order IPTS with the general phasor transforms [17], [21], [27], [40], [98] further reductions of the construction cost and time for RPEVs with narrow-width power rails [22], [23], [25], [26], [28], [41], active EMF cancellations [24], [31], [35], [43], magnetic mirror models for its inductance analysis [36], large lateral tolerances [37], [38], [42], and segmentations of power rails [29], [30], [32], [33], [39]. Throughout the OLEV project, innovative coil designs and roadway construction techniques as well as a reasonably high operating frequency of 20 kHz realized the highest power efficiency of 83% at an output power of 60 kW with a large air-gap of 20 cm and a fairly good lateral tolerance of 24 cm [26]. Moreover, the power rail construction cost of the OLEV, which accounts for more than 80% of the total commercialization cost for RPEVs [69], has been dramatically reduced to at least a third of that of the PATH project. By virtue of the high operating frequency, the power supply current has also been reasonably mitigated by 200 A, and the battery size has been significantly reduced to 20 kWh, which can be further reduced by increasing the length of power supply rails.

Throughout the OLEV project, the first- (1G), second- (2G), third- (3G), upgraded third- (3^+G), and fourth-generation (4G) OLEVs have been developed by KAIST [69] and extensively tested at the test sites at KAIST since 2009, as shown in Fig. 3.

Among them, the 3^+G OLEV has been widely deployed in Korea and firstly commercialized at a 48 km route in Gumi, Korea. In addition, the 3^+G OLEV bus has been newly commercialized in two bus routes, 12 km in length, respectively, in Sejong, Korea since June 2015. In the rest of this section, the new developments of the 5G and 6G OLEVs, which are highly focused on the reduction of the initial investment cost for its commercialization as well as the interoperability between RPEVs and SCEVs to strongly promote the commercialization of RPEVs, will be primarily addressed since the full development history of the 1G, 2G, 3G, 3^+G, and 4G OLEVs were already addressed in a previous review paper [69]. Now, the development of the 5G OLEV, which adopted an ultra-slim

Fig. 3. Deployment status of OLEVs in Korea.

S-type power supply module of 4 cm width to further reduce the power supply rail construction cost and time, is in the final stage of development [41], while that of the 6G OLEV using a new coreless power supply rail for the interoperability between RPEVs and SCEVs is in the early stages of development [84].

A. 5G OLEV

Through the developments of the previous OLEVs, a significant improvement in lateral tolerance as well as a large air-gap, high-power efficiency, lower construction time and cost have been achieved. The construction cost and time of the power supply rail, however, should be further reduced for better commercialization because the construction cost of the power supply rail is critical for deploying the RPEVs and long construction time results in more traffic jams and extra deployment costs.

In order to mitigate these problems, the 5G OLEV adopted an ultra-slim S-type power supply rail for RPEVs with a maximum output power of 22 kW for a flat pick-up, having an air-gap of 20 cm and a lateral tolerance of 30 cm [41]. The S-type power supply rail, where the name “S-type” stems from the front shape of the power supply rail, as shown in Fig. 4(c), has an ultra-slim width of only 4 cm by virtue of the S-type configuration, which has been decreased more than two times compared to that of the I-type power supply module for the 4G OLEV.

Each magnetic pole of the S-type power rail consists of ferrite core plates and power cables, and the adjacent magnetic poles are connected by bottom core plates, as shown in Fig. 4(a). The EMF for pedestrians around the power supply rail can be significantly reduced due to the opposite magnetic polarity of adjacent poles, as shown in Fig. 4(b). The EMF generated from the I-type power supply rail and a flat type pick-up coil set, which is basically the same structure of the proposed S-type one, was as low as 1.5 μT at a distance of 1 m from the power supply rail [41]. Therefore, the S-type one has a similar EMF to the I-type one, which is well below the ICNIRP guideline of 27 μT. Moreover, a large lateral displacement d_{lat} is obtained [41] due to the small width w_t of the S-type power supply rail for a given pick-up width w_p as in

$$d_{\text{lat}} \cong \frac{w_p}{2} - \frac{w_t}{2}. \tag{1}$$

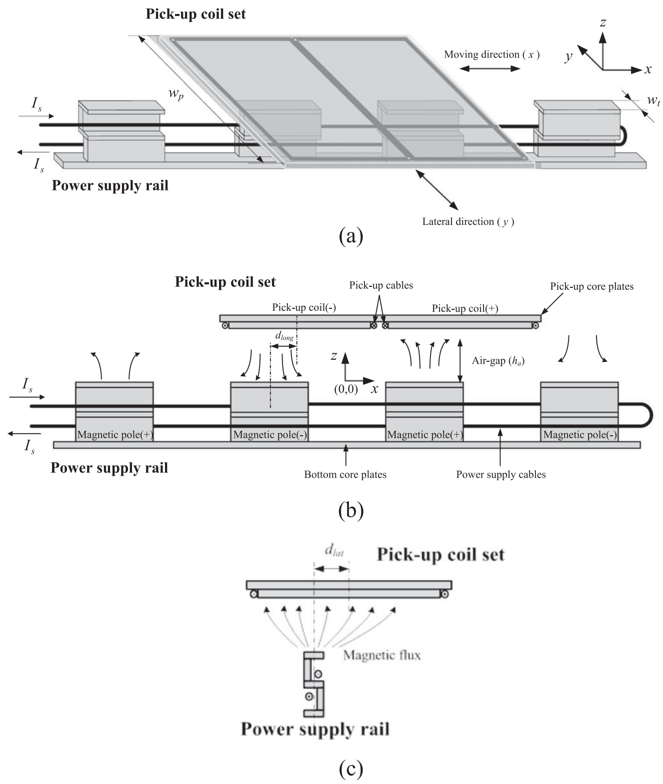

Fig. 4. Proposed ultra-slim S-type power rail and the flat pick-up coil of the IPTS [41]. (a) Bird's eye view. (b) Side view. (c) Front view.

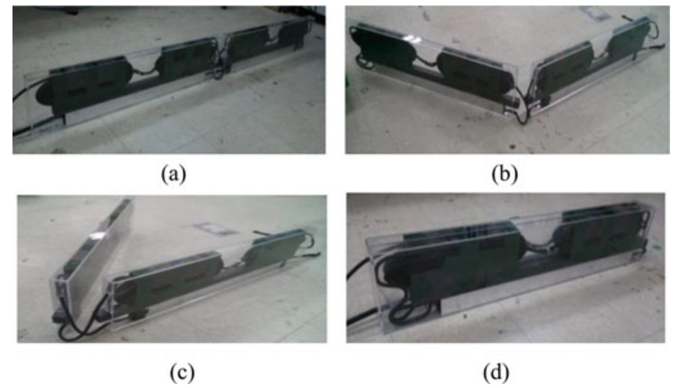

Fig. 6. Fabricated ultra-slim S-type power supply modules [41]. (a) Fully deployed case. (b) One-third folded case. (c) Two-thirds folded case. (d) Completely folded case.

Fig. 7. Aluminum box and capacitor banks for the S-type power supply modules [71]. (a) Separated case. (b) Inserted case.

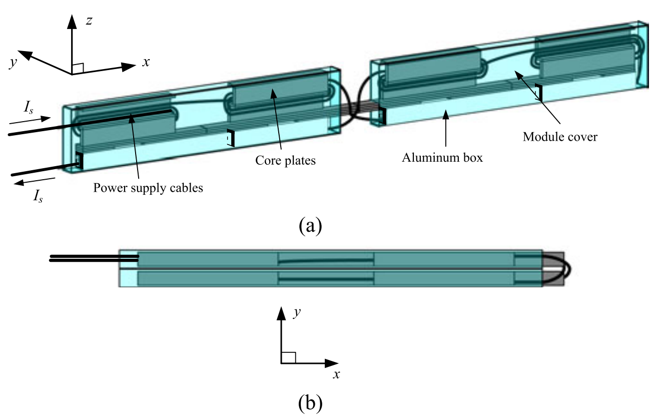

Fig. 5. Configuration of the ultra-slim S-type power supply modules including two magnetic poles [41]. (a) Bird's eye view for two unfolded modules. (b) Top view of a folded module.

From the experimental verifications, a large lateral tolerance of 30 cm at an air gap of 20 cm was experimentally obtained, which is 6 cm larger than that of the I-type power supply rail [41]. The proposed S-type power supply rail adopts a module concept, as shown in Fig. 5(a), and makes it easier to fold itself by virtue of flexible thin power cables. Therefore, no power cable connection is required after being deployed, as shown in Fig. 5(b).

On the other hand, the only demerit of the S-type power supply rails is relatively large self-inductance of a power supply rail compared to previous power supply rails, which can result in large voltage stresses between power supply rails. This is because the structure of the S-type one generally needs a high number of power supply rail turns and this problem, however, can be effectively mitigated by adopting distributed compensation capacitor banks between power supply rails [94]. The S-type power supply module was fabricated, as shown in Fig. 6. The S-type power supply module includes S-type power supply rails, a transparent module cover, and an aluminum box for capacitor banks for better heat transfer to the ground. As shown in Fig. 7, the capacitor bank should be smaller than the aluminum box to be inserted into it and electrically isolated from the aluminum box because aluminum is a conductive material. Moreover, each module, which has two magnetic poles, is serially connected to the capacitor bank installed in an adjacent module in order to mitigate high voltage stress for a capacitor bank due to the large self-inductance of the power supply rail. With the flexible thin power cables having a diameter of 0.9 cm, it is possible to connect the cables for power supply modules at the factory instead of at the construction site, thus avoiding a long construction time, which leads to traffic jams and additional construction costs.

For commercialization, power supply modules should be robust to high humidity as well as repetitive external mechanical impacts for at least 10 years [69]. As a remedy, the S-type power supply module can be filled with epoxy to reinforce the S-type power supply rail and to protect the module from high humidity while the module cover endures external mechanical impacts.

TABLE I
CHARACTERISTICS OF I-TYPE AND S-TYPE POWER SUPPLY RAILS [41]

	I-type (4G OLEV)	S-type (5G OLEV)
Rail width	10 cm	4 cm
Lateral tolerance	24 cm	30 cm
Air-gap	20 cm	20 cm
Output power	27 kW/pick-up	22 kW/pick-up
Efficiency	74% at 27 kW	71% at 22 kW

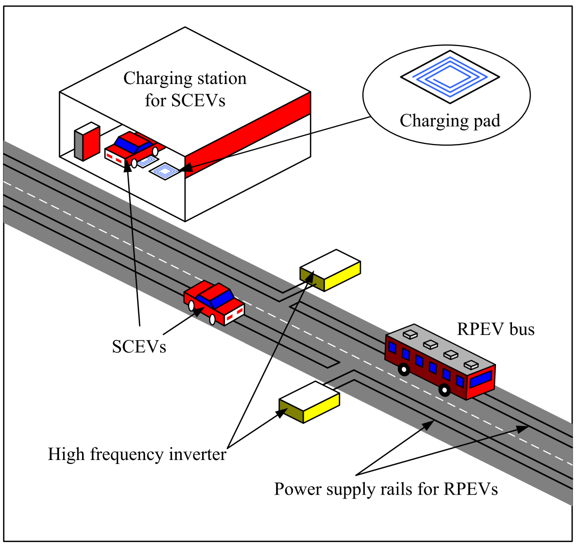

Fig. 8. Ideal concepts for SCEVs compatible with power supply rails for RPEVs [84].

In conclusion, the characteristics of the I-type and S-type power supply rails are summarized, as shown in Table I.

Except for the rail width reduction and lateral tolerance increase, the output power and efficiency of the S-type one are slightly inferior to those of the I-type one, assuming that the pick-up size and ampere-turn of the power supply rail are the same. For readers who are interested in the detailed design issues and experimental verifications for the 5G OLEV of the S-type power supply rail is recommended to refer to [41].

B. 6G OLEV

Although RPEVs are free from the battery problems and are ready for commercialization, RPEVs have not been widely used so far due to the huge initial investment cost. To cope with this problem, we may need strong motivation to build the national infrastructure for RPEVs with public consent. So one of the best deployment scenarios would be that SCEVs are designed to be completely compatible with IPTSs for RPEVs to be wirelessly charged while moving on a road, as shown in Fig. 8, because there is no doubt that SCEVs will be widely deployed all over the world in the near future to replace wired EV chargers due to SCEVs' convenience and safe operation. However, the design considerations of an IPTS for RPEVs are quite different from

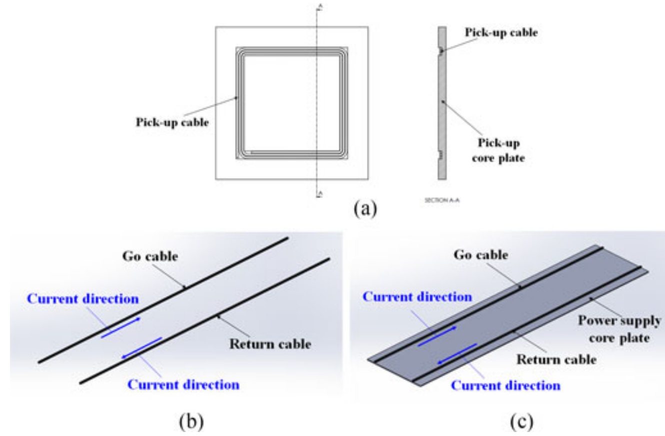

Fig. 9. Conceptual scheme of the proposed coreless power supply rail for both RPEVs and SCEVs [84]. (a) A rectangular pick-up coil for SCEVs in accordance with the SAE J2954. (b) Proposed coreless power supply rail. (c) Conventional power rail used for the 3G and 3G+ OLEVs.

those of SCEVs because the IPTS for RPEVs should meet additional system requirements such as low construction cost and time, low voltage stress, large lateral tolerance, high-power delivery capability, and continuous power delivery while moving on the road.

In order to manage the interoperability issue between RPEVs and SCEVs to the satisfaction of the design goals for RPEVs, the 6G OLEVs, using a new coreless power supply rail, were recently proposed [84]. As shown in Fig. 9, the shape of the proposed coreless power supply rail is basically the same as the U- and W-type power supply rails, which were used for the 3G and 3G + OLEVs, but there is no core plate. Therefore, the proposed coreless power supply rail can generate a uniform magnetic field along a road, and a rectangular pick-up coil determined by the SAE J2954 for SCEVs, as shown in Fig. 9(a), is completely compatible with the power supply rail for RPEVs and continuously gets uniform output power when moving on the road. Moreover, the construction cost and time of the proposed coreless power supply rails can be further reduced with the elimination of concrete forming works, which have been used for protecting core plates from external impacts, compared to the conventional with-core power supply rails because the concretes are no more needed for coreless rails and the concrete-forming works require at least 2 weeks for its hardening. Meanwhile, the large voltage stresses on both the compensation capacitor bank and distributed power supply rail V_{l1} are a unique feature of RPEVs, and this is one of the main reasons that the operating frequency is limited by around 20 kHz [69] because the voltage stress is directly proportional to its operating frequency f_s as well as its power supply current I_s as follows:

$$V_{l1} = j\omega_s L_{l1} I_s \quad \because \omega_s = 2\pi f_s \tag{2a}$$

$$\frac{\partial V_{l1}}{\partial x} = j\omega_s I_s \frac{\partial L_{l1}}{\partial x}. \tag{2b}$$

In accordance with the magnetic mirror model [36], however, it is well known that the self-inductance of a power supply rail

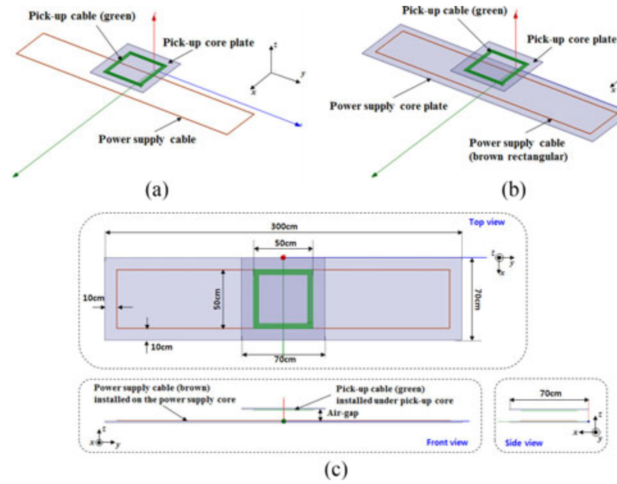

Fig. 10. Maxwell simulation models for the proposed coreless power supply rail with a rectangular pick-up [84]. (a) Bird's eye view of the proposed coreless power supply rail. (b) Bird's eye view of the conventional with-core power supply rail. (c) Dimensions for the simulation models.

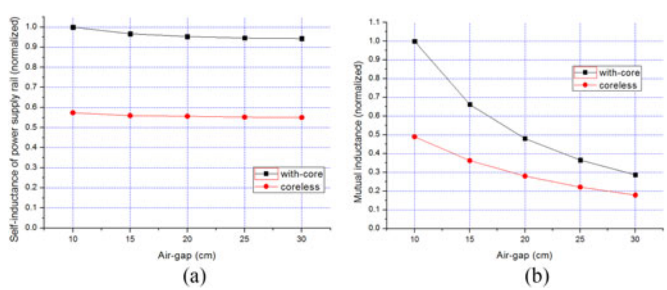

Fig. 11. Self-inductance of a power rail with/without core plates along to an air-gap [114]. (a) Self-inductance and (b) mutual inductance variations.

with core plates can become two times that without core plates when core plates are infinitely long and its relative permeability is infinite; hence, it is expected that the proposed coreless power supply rail will have about a half of its previous voltage stress due to its reduced inductance so that the operating frequency can be increased from 20 to 85 kHz to meet the SAE J2954 standard for SCEVs with only about two times the voltage stress compared to that of 20 kHz for a given rail current. Moreover, it is also expected that the proposed coreless power supply rail can guarantee a large lateral tolerance compared to the conventional with-core power supply rails because the self-inductance variation of the pick-up coil along to lateral displacements is small enough to be negligible when a coreless power supply rail is used. In order to validate those unique characteristics of the proposed coreless power supply rail, two simulation models, which are with-core and coreless power supply rails with a rectangular pick-up for SCEVs, are proposed, as shown in Fig. 10.

From the simulation results, it is found that the self-inductance of the proposed coreless rail is about half that of the conventional with-core power supply rail, as shown in Fig. 11(a). At the same time, the mutual inductance of the pro-

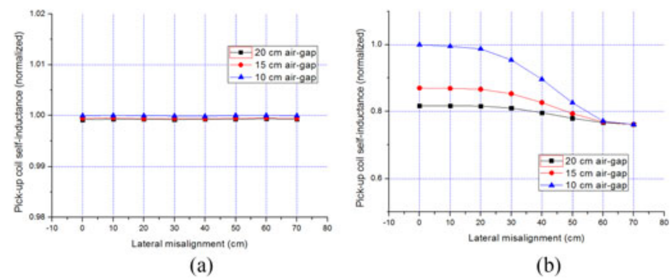

Fig. 12. Self-inductance of the pick-up coil along lateral displacements [84]. (a) Proposed coreless rail. (b) Conventional with-core rail.

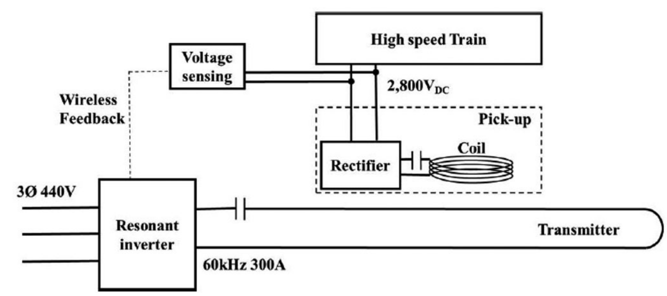

Fig. 13. Configuration of the IPTS for a high-speed train [85].

posed coreless power rail also becomes half that of the conventional with-core power rail, as shown in Fig. 11(b).

Moreover, the self-inductance variation of a pick-up coil with the proposed coreless power supply rail is negligible along lateral displacements, as shown in Fig. 12, which means that the proposed coreless power supply rail can guarantee a larger lateral tolerance of RPEVs and SCEVs compared to the conventional with-core power supply rail [84].

IV. Research Trends of RPEVs by Other Research Teams

Among other research teams, a couple of active research teams such as Auckland, Bombardier, and ORNL teams are not addressed in this section since the previous review paper already dealt with important design considerations of their WPTSs for RPEVs [69]. In this section, therefore, three research teams, which have reached the development level of full-sized WPTSs for RPEVs, are newly addressed in this paper.

A. Korea Railroad Research Institute (KRRI) Team

Since 2012, the KRRI team has been developing IPTSs for a high-speed train and achieved a maximum output power of 820 kW with a system efficiency of 83% at an air-gap of 5 cm [85]. For the small pick-up size as well as cost reduction in the IPTS, an operating frequency of 60 kHz, which is three times of that used for the 1G, 2G, 3G, 4G, and 5G OLEVs, was adopted while a single-phase power system was used instead of a three-phase power system due to its simple control and low-cost characteristics, as shown in Fig. 13. To realize the 1 MW level high-frequency inverter, five 200 kW level full-bridge pulse

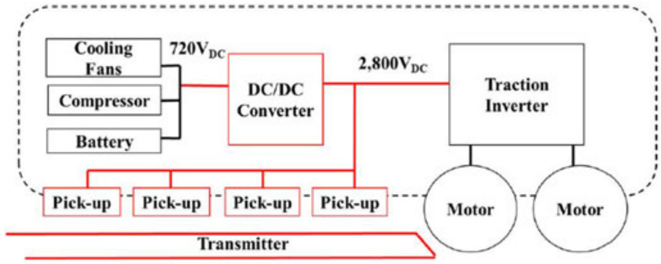

Fig. 14. Block diagram of the high-speed train with the IPTS [85].

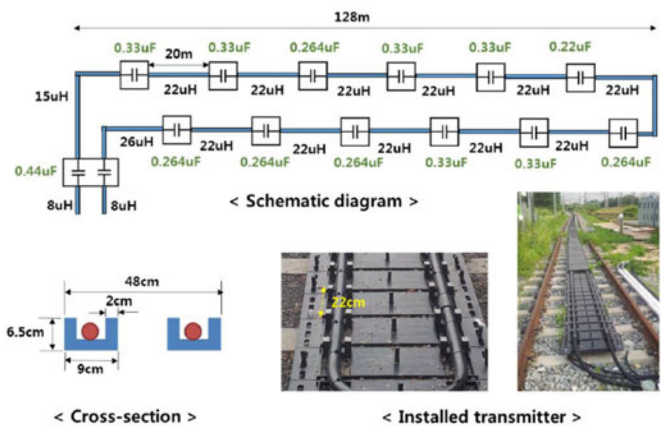

Fig. 15. Schematic diagram and photos of the transmitter for a high-speed train [85].

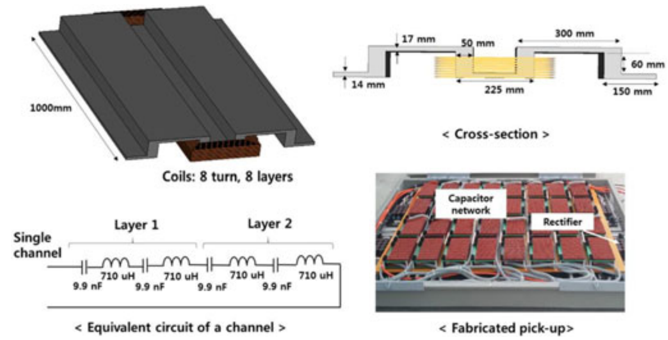

Fig. 16. Schematic diagram and photos of the pick-up for a high-speed train [85].

Fig. 17. View of the high-speed train with the IPTS [85].

amplitude modulation resonant inverters using insulated gate bipolar transistor (IGBT) modules were connected in parallel for cost effectiveness [85].

Moreover, four pick-up sets, i.e., 200 kW for each pick-up set, are connected in parallel, and the output voltage of the pick-up sets is directly controlled by resonant inverter currents through the voltage sensor and wireless feedback systems to rapidly adjust the traction inverter input voltage of 2800 V_{DC}, as shown in Fig. 14, without any additional regulator and batteries, which would lead to large volume, weight, and cost problems on the pick-up side [85].

As mentioned in the previous section on the 6G OLEV, the large voltage stress on both the compensation capacitor banks and power supply rails becomes a significant problem of the high-power level IPTS using a high operating frequency of more than 20 kHz. As a remedy for this problem, it is essential to use distributed compensation capacitors, and they are connected in series with the transmitter and pick-up coils to effectively reduce the voltage stress between power cables, as shown in Figs. 15 and 16. The structure of the power supply rail and pick-up used for the IPTS is basically the same as the 3G and 3^+G OLEVs because these structures can guarantee several significant advantages such as low construction cost and time, high-power transfer capability, continuous power transfer along a rail, and low EMF characteristics. For the system integration test, KRRI made a 128-m-long power supply rail, as shown in Fig. 17. From this integration test, the high-speed train using the IPTS successfully operated and accelerated to a speed of 10 km/h.

B. Endesa Research Team

Since April 2013, Endesa has been involved in the vehicle initiative consortium for transport operation and road inductive application (VICTORIA) project and has adopted the triple charging technologies such as conventional plug-in, stationary, and dynamic charging systems based on an IPTS for RPEVs, as shown in Fig. 18. Hence, RPEVs can be charged by a plug-in charger when parked at a bus terminal during night, and during the daytime, RPEVs can be partially charged at wireless charging bus stops and bus lanes equipped with power supply rails while moving over them to extend the vehicles' driving ranges [86]. For stationary and dynamic charging, Endesa did not adopt multiple small pads but rather a power supply rail to guarantee several advantages such as its continuous power transfer, low construction cost and time, and simple control characteristics; with a rectangular pick-up, the U-type power supply rail, which had been used for the 2G OLEVs developed by KAIST in 2011 [69], was used for an interoperability between stationary and dynamic charging, as shown in Fig. 19. For demonstration purposes, as shown in Fig. 20, an RPEV with a maximum power transfer of 50 kW has been deployed and operated in the 10 km bus route of the Number 16 bus in Malaga, Spain since December 2014.

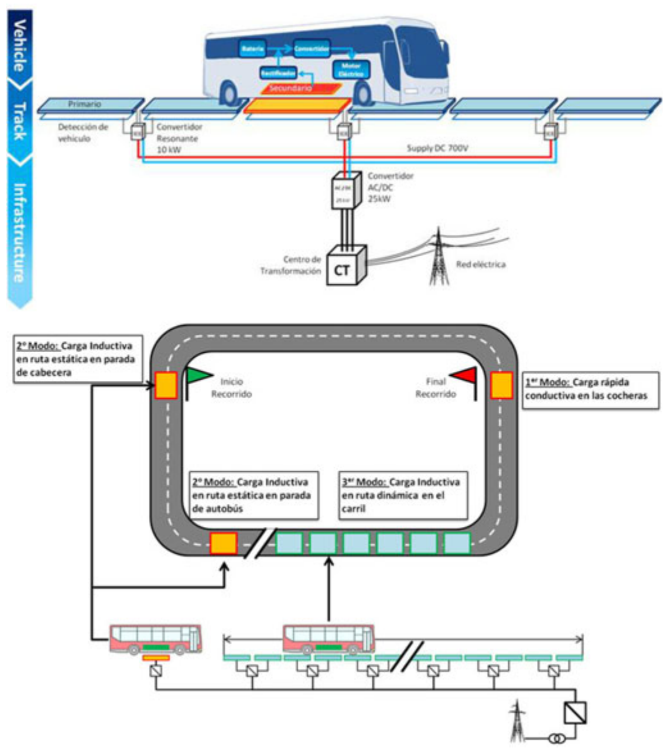

Fig. 18. General concept of the VICTORIA project applying the triple charging technologies to RPEVs [86].

Fig. 19. U-type power rail (left) and rectangular pick-up (right) used for the RPEV developed by the VICTORIA project [87].

Fig. 20. RPEV developed by the VICTORIA project for triple charging [88].

Fig. 21. Scheme of ten-segmented power rails in Malaga, Spain [88].

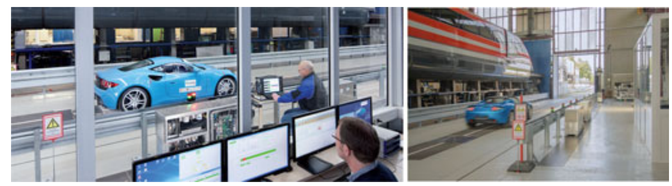

Fig. 22. INTIS test center having a 25-m-long track for the IPTS of SCEVs and RPEVs [90].

Within the total bus route of 10 km, ten-segmented power supply rails were installed along the route, totaling 300 m in length, where the eight-segmented power supply rails had an interval of 12.5 m for dynamic charging, and the interval between other two-segmented power supply rails was 300 m for stationary charging, as shown in Fig. 21. Moreover, a self-guided control system, which automatically controls the steering wheel to follow the center of a road in the same way as in the 1G OLEV, has been adopted to minimize lateral displacements for its efficient power transfer [88]. Unfortunately, there is not much open access information about the Endesa team's works compared to that of the other research teams.

C. Integrated Infrastructure Solution (INTIS) Research Team

The INTIS has been investigating the IPTS for both SCEVs and RPEVs to provide engineering services and consulting from developments to field tests since 2011 [89]. Now, INTIS has its own 25-m-long power supply rail in a test center in Lathen, Germany, as shown in Fig. 22, and the test center can be used to evaluate IPTSs for SCEVs and RPEVs from the component level to the completed system level.

Based on a single-phase power system, the test power supply rail of the IPTS for SCEVs and RPEVs is available for tests up to a maximum output power of 200 kW at an operating frequency of up to 35 kHz while the double U-type power supply rail, which has two U-type power rails in parallel, is adopted at the test center, as shown in Fig. 23. So far, INTIS has developed two IPTSs for SCEVs and RPEVs [91], which used an operating frequency of 30 kHz for the maximum output power of 30 kW at an air-gap of 10 cm, as shown in Fig. 24.

V. Few Technical Issues of RPEV

As an alternative to the long power supply rail scheme [69], which has been widely used for the wireless powering of RPEVs due to its strong advantages, a lumped IPTS including many small power pads was introduced, where the size of a power

Fig. 23. Test frame for a pick-up (left) and double U-type power supply rail (right) used in the test center [90].

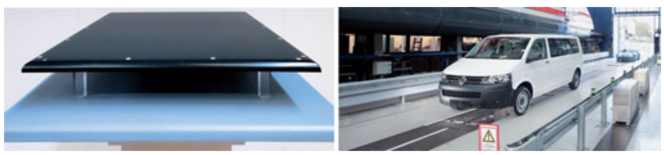

Fig. 24. Power supply rails and pick-up coils for SCEVs (left) and RPEVs (right) developed by INTIS [91].

pad is almost the same with that of a pick-up coil to avoid unwanted energizing and leakage magnetic fluxes [54]. In this section, a few important technical issues, such as coil structures, power supply schemes, and segmentation switching techniques of a lumped IPTS for RPEVs, are addressed, which were not significantly dealt with in our previous review paper [69].

A. Coil Structures

In general, a lumped IPTS utilizes a string of primary coils deployed under the road surface at discrete locations to transfer power inductively to a secondary coil (or pick-up) onboard a moving EV. The coupling coefficient between a primary coil and pick-up coil is a fundamental parameter in determining the power transfer efficiency and power transfer capability of any IPTS; it depends not only on the coil distance, which changes during the vehicle motion for the dynamic wireless power transfer (DWPT), but also on the misalignment and shape of the coils [92]. There are two main classes of coils: unipolar and bipolar. A unipolar coil is characterized by the presence of only one magnetic pole in each coil face. The coil has simple topologies, such as circular, square, and spiral. The flux lines leave the coil face with a north pole and enter into the coil face with a south pole going around the coil edge. A bipolar coil has a more complex topology, with the coil faces having both north and south poles. In this case, the flux lines leave the region of the coil face with the north pole and enter into the region with the south pole on the same coil face. Flux lines are, hence, confined in the space over (and under) the coil, thereby increasing the coupling coefficient with an overhead bipolar coil and reducing the concern about field shielding. In both the coil classes, leaning the coil against a flat ferrite core contributes to increasing the coupling coefficient.

An effective bipolar coil topology has the double-D (DD) shape, as shown in Fig. 25(a), where the D geometry is squared. By this topology, the coupling characteristic of a unipolar two-coil coupling is greatly outperformed. A DD coil is made of two

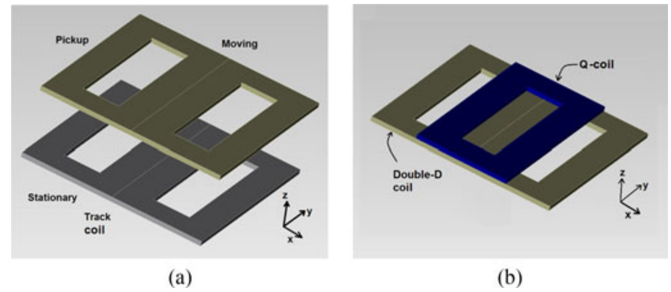

Fig. 25. Simulation models of (a) double-D (DD) coils and (b) double-D quadrature (DDQ) pick-up coil.

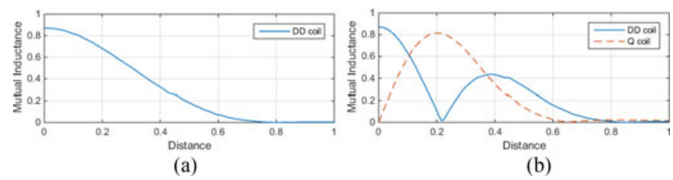

Fig. 26. Mutual inductance plots: (a) motion in the *y* direction, and (b) motion in the *x* direction (*x, y* scales are arbitrary).

D-shaped sections placed back-to-back in the same plane. The sections are electrically connected to produce opposite magnetic polarities over their faces. When a DD-shaped pick-up is superimposed on a primary DD coil, the flux generated by each section of the primary coil is linked with the corresponding section of the pick-up and the voltage at the pick-up terminals is the sum of the voltages induced in its two sections.

With circular two-coil coupling, the profile of the mutual inductance has a radial symmetry with respect to the distance from the center of a coil. Instead, the profile of the mutual inductance of a DD two-coil coupling does not have such a symmetry and is commonly given along two orthogonal directions: one orthogonal to the back-to-back side of the DD coil, denoted as the *x* direction, and the other one parallel to the back-to-back side of the DD coil, denoted as the *y* direction. The *y*-direction mutual inductance has the smoothly varying profile shown in Fig. 26(a), similar to that of a circular two-coil coupling. Instead, the *x*-direction mutual inductance drops to zero even when the pick-up is moving over the primary DD coil. Indeed, as a pick-up moves to the *x*-direction from the primary coil position, the fluxes generated by the two sections of the primary DD coil and linked with each section of the DD-shaped pick-up are equal and of opposite signs. The relevant profile of the mutual inductance is shown in Fig. 26(b).

At the distance of zero-mutual inductance, the voltage induced in the pick-up as well as the power transfer is zero. This particular pick-up position is called a null power point.

The presence of the null power point severely impairs the power transfer capability of a DWPT system when the pick-up travels along the *x* direction; instead, if the pick-up travels along the *y* direction, possibly with a small misalignment in the *x* direction, there is no null power point; in practice, however, the condition of small misalignment is difficult to maintain along

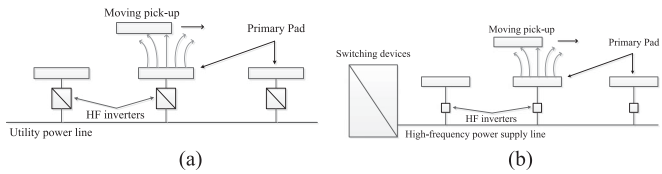

Fig. 27. DWPT primary coil supply arrangements.

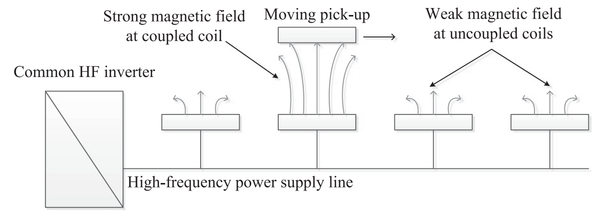

Fig. 28. Conceptual layout of the reflexive segmentation.

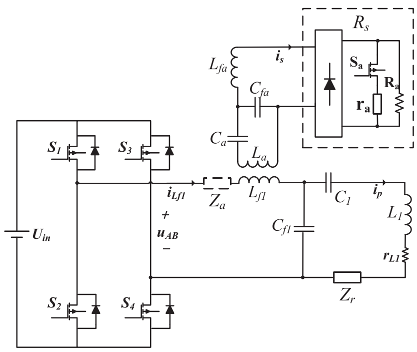

Fig. 29. Primary coil current regulation circuit.

the full travel so that the motion along the y direction is also impaired by the presence of the null power point. To overcome such a drawback, an additional coil is placed in the center of the pick-up, as shown in Fig. 25(b). This coil, named a quadrature coil (Q-coil), captures the flux produced by the primary DD coil around the null power point of the DD-shaped pick-up so that the pick-up as a whole, when moving over a primary coil, always has the capability of receiving power from it. The dashed line in Fig. 26(b) shows the profile of the mutual inductance of the Q-coil; its maximum is just in correspondence of the drop of the mutual inductance of the DD-shaped pick-up (solid line) and has a magnitude comparable to that of the DD-shaped pick-up so that the power it receives compensates almost entirely for the null power point of the DD-shaped pick-up.

B. Power Supply Scheme

At a given instant, many EVs can move on the road, and their pick-ups are coupled with different primary coils. In general, however, some primary coils remain uncoupled. If energized, they are affected by losses and, furthermore, constitute a hazard for the nearby people and environment due to the generated magnetic field. To deal with this issue, only the primary coils covered by pick-ups are energized and execute the power transfer. This technique is termed primary segmentation. There are basically two supply arrangements that implement segmentation. One utilizes the straightforward approach of equipping each primary coil with an individual inverter, as shown in Fig. 27(a). The inverter is turned ON and OFF when the presence and absence of an overhead pick-up are detected. The merits of the arrangement are the usage of low-power inverters and separate resonant compensations of each primary coil, with an improvement in reliability and performance of the DWPT system. The drawback of the arrangement is the deployment of a large number of inverters and sensing devices.

The other arrangement consists of supplying a string of primary coils with a common inverter and in endowing each coil with a switching device, as shown in Fig. 27(b). The switching device is turned on and off when the presence and absence of an overhead pick-up is detected. The merit of the arrangement is the usage of only one inverter; its shortcoming is the deployment of a large number of sensing and switching devices.

C. Segmentation Switching Technique

Implementation of segmentation by means of the previously described arrangements increases the cost and complexity of the DWPT systems. To cope with these inconveniences, a different solution, reflexive segmentation, has been proposed in [93]. It still uses a common inverter for the supply of a string of primary coils but does not make use of sensing and switching devices. As for the arrangement in Fig. 27(b), the primary coils are connected in parallel to the inverter output, as shown in Fig. 28.

The combined effect of the self-inductance of the primary coils, which are not compensated for by a capacitor in this proposal, and the high-frequency supply makes the coil impedance very high under uncoupled conditions. Therefore, the current flowing in the uncoupled primary coils is low, and the magnetic field generated by them is weak. When a primary coil is coupled to a pick-up, the impedance of the latter one is reflected to the primary coil. By setting up the pick-up with a reactive network that, when reflected is able to compensate for the reactance of the primary coil, the impedance seen from the inverter is dramatically reduced. Consequently, as the current in the coupled primary coil increases substantially, the magnetic field produced by it becomes much stronger and electric power is transferred to the coupled pick-up.

In a similar way, reactive power compensation networks (RPCN) have been introduced to compose the energy transmitting pad-array in the primary side. These RPCNs are excited by a common inverter, which is quite cost-effective. The excitation current flowing into every RPCN could be automatically built up when the pickup coil is coupled or partly coupled. Since the LCC compensation scheme, which has been widely used due to its current source characteristics for the primary side, is adopted in RPCNs, constant HF currents constantly flow into the primary coil regardless of the existence of the pick-up, and this problem could lower its power transfer efficiency. As a remedy for this problem, an auxiliary LCC compensation network to selectively change reflected impedance Z_a is adopted to regulate the RMS of the primary coil current with the circuit structure, as shown in Fig. 29.

In the auxiliary circuit, R_a is a high resistance, which ranges from 10 to 100 k ohm, and r_a is the turn-on resistance of MOSFET S_a. The output impedance of the auxiliary LCC network is R_s, which is comprised of R_a, r_a, and the internal resistance of the rectifier bridge. There are two operation modes in the auxiliary LCC network: short-circuit mode and open-circuit mode. When the pickup coil is coupled or partly coupled with the primary coil, the regulation circuit operates in the short-circuit mode to minimize the reflected impedance Z_a so that energy is transferred from the primary side to the pickup side. On the other hand, the regulation circuit operates in the open-circuit mode to maximize the reflected impedance Z_a so that its system efficiency increases and unwanted leakage magnetic fluxes decrease with low inverter output current I_{Lf1}.

VI. Conclusion

As a follow-up to the previous review paper that dealt with a full history of WPTSs for RPEVs from its advent in the 1890s to its modern status [69], recent studies over the past couple of years have been newly summarized in this review paper. For the more than 100-year history of RPEVs, the power transfer capacity, efficiency, lateral tolerance, EMF, air-gap, size, weight, and cost of the WPTSs have been significantly improved by virtues of innovative semiconductor switches, better coil designs, enhanced roadway construction techniques, and higher operating frequency. Thus, there is no doubt that RPEVs are becoming viable solutions for future transportation and that the 6G OLEV, reducing infrastructure cost for commercialization and increasing the interoperability between RPEVs and SCEVs, will be an especially strong candidate for the near-future widespread use of RPEVs in public transportation.

References

[1] M. Hutin and M. Leblanc, “Transformer system for electric railways,” U.S. Patent 527 857, 1894.

[2] S. E. Schladover, “Systems engineering of the roadway powered electric vehicle technology,” presented at the 9th Int. Electric Veh. Symp., 1988.

[3] J. G. Bolger, “Roadway power and control system for inductively coupled transportation system,” U.S. Patent 4 836 344, 1989.

[4] M. Eghtesadi, “Inductive power transfer to an electric vehicle-an analytical model,” in *Proc. IEEE 40th Veh. Technol. Conf.*, 1990, pp. 100–104.

[5] K. W. Klontz, D. M. Divan, D. W. Novotny, and R. D. Lorenz, “Contactless battery charging system,” U.S. Patent 5 157 319, 1992.

[6] K. W. Klontz, D. M. Divan, D. W. Novotny, and R. D. Lorenz, “Contactless coaxial winding transformer power transfer system,” U.S. Patent 5 341 280, 1994.

[7] J. G. Bolger, “Urban electric transportation systems: The role of magnetic power transfer,” in *Proc. IEEE WESCON*, 1994, pp. 41–45.

[8] California PATH Program, “Roadway powered electric vehicle project track construction and testing program phase 3D,” Univ. California, Berkeley, CA, USA, California PATH Res. Paper UCB-ITS-PRR-94-07, Mar. 1994.

[9] K. W. Klontz, D. M. Divan, D. W. Novotny, and R. D. Lorenz, “Contactless power delivery system for mining applications,” *IEEE Trans. Ind. Appl.*, vol. 31, no. 1, pp. 27–35, Jan. 1995.

[10] KAIST OLEV team, “Feasibility studies of on-line electric vehicle (OLEV) project,” KAIST Internal Rep., Aug. 2009.

[11] N. P. Suh, D. H. Cho, and C. T. Rim, “Design of on-line electric vehicle (OLEV),” in *Proc. Plenary Lecture CIRP Des. Conf.*, 2010, pp. 3–8.

[12] S. W. Lee, J. Huh, C. B. Park, N. S. Choi, G. H. Cho, and C. T. Rim, “On-line electric vehicle (OLEV) using inductive power transfer system,” in *Proc. IEEE Energy Convers. Congr. Expo.*, 2010, pp. 1598–1601.

[13] J. Huh, S. W. Lee, C. B. Park, G. H. Cho, and C. T. Rim, “High performance inductive power transfer system with narrow rail width for on-line electric vehicles,” in *Proc. IEEE Energy Convers. Congr. Expo.*, 2010, pp. 647–651.

[14] C. T. Rim, “The difficult technologies in wireless power transfer,” *Trans. Korean Inst. Power Electron.*, vol. 15, no. 6, pp. 32–39, Dec. 2010.

[15] S. W. Lee, C. B. Park, J. G. Cho, G. H. Cho, and C. T. Rim, “Ultra slim U & W power supply and pick-up coil design for OLEV,” in *Proc. Korean Inst. Power Electron. (KIPE) Annu. Summer Conf.*, 2010, pp. 353–354.

[16] G. H. Jung *et al.*, “Non-touch inductive power transfer system for OLEV,” in *Proc. Korean Inst. Elect. Eng. (KIEE) Annu. Summer Conf.*, 2010, pp. 1054–1055.

[17] C. B. Park, S. W. Lee, and C. T. Lim, “Dynamic phasor transformation using complex Laplace transformation,” in *Proc. Korean Inst. Power Electron. (KIPE) Annu. Fall Conf.*, 2010, pp. 46–47.

[18] G. H. Jung *et al.*, “Power supply and pick-up system for OLEV,” in *Proc. Korean Inst. Power Electron. (KIPE) Annu. Summer Conf.*, 2010, pp. 218–219.

[19] J. Huh, W. Y. Lee, J. G. Cho, G. H. Cho, and C. T. Rim, “A study on current source-transformer resonance inductive power transfer system,” in *Proc. Korean Inst. Power Electron. Annu. Summer Conf.*, 2010, pp. 355–356.

[20] C. T. Rim, “Electric vehicle system,” Patent WO 2010 076976, 2010.

[21] C. T. Rim, “Unified general phasor transformation for AC converters,” *IEEE Trans. Power Electron.*, vol. 26, no. 9, pp. 2465–2745, Sep. 2011.

[22] S. W. Lee, C. B. Park, J. G. Cho, G. H. Cho, and C. T. Rim, “Ultra slim supply and pick-up coils for on-line electric vehicles (OLEV),” *Trans. Korean Inst. Power Electron. (KIPE),* vol. 16, no. 3, pp. 274–282, Aug. 2011.

[23] J. Huh and C. T. Rim, “KAIST wireless electric vehicles—OLEV,” presented at the JSAE Annu. Congr., 2011.

[24] S. W. Lee *et al.*, “Active EMF cancellation method for I-type pick-up of on-line electric vehicles (OLEV),” in *Proc. IEEE Appl. Power Electron. Conf. Expo.*, 2011, pp. 1980–1983.

[25] J. Huh, W. Y. Lee, G. H. Cho, B. H. Lee, and C. T. Rim, “Characterization of novel inductive power transfer systems for on-line electric vehicles (OLEV),” in *Proc. IEEE Appl. Power Electron. Conf. Expo.*, 2011, pp. 1975–1979.

[26] J. Huh, S. W. Lee, W. Y. Lee, G. H. Cho, and C. T. Rim, “Narrow-width inductive power transfer system for on-line electrical vehicles (OLEV),” *IEEE Trans. Power Electron.*, vol. 26, no. 12, pp. 3666–3679, Dec. 2011.

[27] S. W. Lee, C. B. Park, and C. T. Rim, “An analysis of DQ inverter for wireless power transfer by complex Laplace-phasor transformation,” in *Proc. Korean Inst. Power Electron. Annu. Summer Conf.*, 2011, pp. 192–193.

[28] N. P. Suh, D. H. Cho, G. H. Cho, J. G. Cho, C. T. Rim, and S. H. Jang, “Ultra slim power supply and collector device for electric vehicle,” Patent KR 1010406620000, 2011.

[29] S. Z. Jeon, D. H. Cho, C. T. Rim, and G. H. Jeong, “Load-segmentation-based full bridge inverter and method for controlling same,” Patent WO 2011 078424, 2011.

[30] S. Z. Jeon, D. H. Cho, C. T. Rim, and G. H. Jeong, “Load-segmentation-based 3-level inverter and method for controlling the same,” Patent WO 2011 078425, 2011.

[31] N. P. Suh *et al.*, “Monorail type power supply device for electric vehicle including EMF cancellation apparatus,” Patent WO 2011 046374, 2011.

[32] N. P. Suh *et al.*, “Space division multiplexed power supply and collector device,” Patent WO 2011 152678, 2011.

[33] N. P. Suh *et al.*, “Cross-type segment power supply,” Patent WO 2011 152677, 2011.

[34] J. Huh and C. T. Rim, “A new coil set with core for magnetic resonant systems,” in *Proc. Korean Inst. Power Electron. Annu. Summer Conf.*, 2012, pp. 625–626.

[35] N. P. Suh, S. H. Jang, D. H. Cho, G. H. Cho, Chun T. Rim, S. W. Lee, and C. B. Park, “EMI cancellation device in power supply and collector device for magnetic induction power transmission,” Patent WO 2011 149263, 2012.

[36] W. Y. Lee *et al.*, “Finite-width magnetic mirror models of mono and dual coils for wireless electric vehicles,” *IEEE Trans. Power Electron.*, vol. 28, no. 3, pp. 1413–1428, Mar. 2013.

[37] C. T. Rim, “Trend of roadway powered electric vehicle technology,” *Korean Inst. Power Electron. Mag.*, vol. 18, no. 4, pp. 45–51, Aug. 2013.

[38] C. T. Rim, “The development and deployment of on-line electric vehicles (OLEV),” presented at the IEEE Energy Convers. Congr. Expo., 2013.

[39] Su Y. Choi, J. Huh, W. Y. Lee, S. W. Lee, and C. T. Rim, "New cross-segmented power supply rails for roadway powered electric vehicles," *IEEE Trans. Power Electron.*, vol. 28, no. 12, pp. 5832–5841, Dec. 2013.

[40] S. Lee, B. Choi, and C. T. Rim, "Dynamics characterization of the inductive power transfer system for on-line electric vehicles (OLEV) by laplace phasor transform," *IEEE Trans. Power Electron.*, vol. 28, no. 12, pp. 5902–5909, Dec. 2013.

[41] S. Y. Choi, B. W. Gu, S. Y. Jeong, and C. T. Rim, "Ultra slim S-type power supply rails for roadway-powered electric vehicles," *IEEE Trans. Power Electron.*, vol. 30, no. 11, pp. 6456–6468, Jun. 2015.

[42] S. Y. Choi, J. Huh, W. Y. Lee, J. G. Cho, and C. T. Rim, "Asymmetric coil sets for wireless stationary EV chargers with large lateral tolerance by dominant field analysis," *IEEE Trans. Power Electron.*, vol. 29, no. 12, pp. 6406–6420, Feb. 2014.

[43] S. Y. Choi, B. W. Gu, S. W. Lee, W. Y. Lee, J. Huh, and C. T. Rim, "Generalized active EMF cancel methods for wireless electric vehicles," *IEEE Trans. Power Electron.*, vol. 29, no. 11, pp. 5770–5783, Nov. 2014.

[44] M. Budhia, G. A. Covic, and J. T. Boys, "Design and optimization of magnetic structures for lumped inductive power transfer systems," *IEEE Trans. Power Electron.*, vol. 26, no. 11, pp. 3096–3108, Nov. 2011.

[45] M. Budhia, G. A. Covic, and J. T. Boys, "A new magnetic coupler for inductive power transfer electric vehicle charging systems," in *Proc. 36th Annu. Conf. IEEE Ind. Electron. Soc.*, Nov. 2010, pp. 2487–2492.

[46] M. Budhia, J. T. Boys, G. A. Covic, and C.-Y. Huang, "Development of a single-sided flux magnetic coupler for electric vehicle IPT charging systems," *IEEE Trans. Ind. Electron.*, vol. 60, no. 1, pp. 318–328, Jan. 2013.

[47] G. A. Covic, L. G. Kissin, D. Kacprzak, N. Clausen, and H. Hao,"A bipolar primary pad topology for EV stationary charging and highway power by inductive coupling," in *Proc. IEEE Energy Convers. Congr. Expo.*, Sep. 2011, pp. 1832–1838.

[48] M. Budhia, G. A. Covic, J. T. Boys, and C.-Y. Huang, "Development and evaluation of single sided flux couplers for contactless electric vehicle charging," in *Proc. IEEE Energy Convers. Congr. Expo.*, Sep. 2011, pp. 614–621.

[49] A. Zaheer, D. Kacprzak, and G. A. Covic, "A bipolar receiver pad in a lumped IPT system for electric vehicle charging applications," in *Proc. IEEE Energy Convers. Congr. Expo.*, Sep. 2012, pp. 283–290.

[50] G. A. Covic, J. T. Boys, M. Kissin, and H. Lu, "A three-phase inductive power transfer system for roadway power vehicles," *IEEE Trans. Ind. Electron.*, vol. 54, no. 6, pp. 3370–3378, Dec. 2007.

[51] C. S. Wang, O. H. Stielau, and G. A. Covic, "Design considerations for a contactless electric vehicle battery charger," *IEEE Trans. Ind. Electron.*, vol. 52, no. 5, pp. 1308–1314, Oct. 2005.

[52] J. T. Boys, G. A. Covic, and A.W. Green, "Stability and Control of inductively coupled power transfer systems," *Proc. Inst. Elect. Eng. —Elect. Power Appl.*, vol. 147, no. 1, pp 37–43, Jan. 2000.

[53] C. S. Wang, G. A. Covic, and O. H. Stielau, "Power transfer capability and bifurcation phenomena of loosely coupled inductive power transfer systems," *IEEE Trans. Ind. Electron.*, vol. 51, no. 1, pp. 148–157, 2004.

[54] G. A. Covic and J. T. Boys, "Modern trends in inductive power transfer for transportation applications," *IEEE J. Emerg. Sel. Topics Power Electron.*, vol. 1, no. 1, pp. 28–41, Mar. 2013.

[55] J. Meins and S. Carsten, "Transferring energy to a vehicle," Patent WO 2010 000494, 2010.

[56] J. Meins and K. Vollenwyder, "System and method for transferring electrical energy to a vehicle," Patent WO 2010 000495, 2010.

[57] K. Vollenwyder, J. Meins, and C. Struve, "Inductively receiving electric energy for a vehicle," Patent US 0055751, 2012.

[58] M. Zengerle, "Transferring electric energy to a vehicle using a system which comprises consecutive segments for energy transfer," U.S. Patent 0217112, 2012.

[59] K. Vollenwyder and J. Meins, "Producing electromagnetic fields for transferring electric energy to a vehicle," U.S. Patent 8544622, 2013.

[60] R. Czainski, J. Meins, and J. Whaley, "Transferring electric energy to a vehicle by induction," U.S. Patent 0248311, 2013.

[61] J. Meins, "German activities on contactless inductive power transfer," presented at the IEEE Energy Convers. Congr. Expo., 2013.

[62] Latest News of Development of Roadway Powered Electric Vehicles for Bombardier. (2016). [Online]. Available: http://primove.bombardier.com/media/news/

[63] O. C. Onar, J. M. Miller, S. L. Campbell, C. Coomer, C. P. White, and L. E. Seiber, "A novel wireless power transfer for in-motion EV/PHEV charging," in *Proc. IEEE Applied Power Electron. Conf. Expo.*, 2013, pp. 3073–3080.

[64] J. M. Miller, O. C. Onar, and P. T. Jones, "ORNL developments in stationary and dynamic wireless charging," presented at the IEEE Energy Convers. Congr. Expo., 2013.

[65] J. Huh, W. Y. Lee, S. Y. Choi, G. H. Cho, and C. T. Rim, "Explicit static circuit model of coupled magnetic resonance system," *IEEE Energy Convers. Congr. Expo. Asia*, May 2011, pp. 2233–2240.

[66] J. Huh, W. Y. Lee, S. Y. Choi, G. H. Cho, and C. T. Rim, "Frequency-domain circuit model and analysis of coupled magnetic resonance systems," *J. Power Electron.*, vol. 13, no. 2, pp. 275–286, Mar. 2013.

[67] E. S. Lee, J. Huh, X. V. Thai, S. Y. Choi, and C. T. Rim, "Impedance transformers for compact and robust coupled magnetic resonance systems," in *Proc. IEEE Energy Convers. Congr. Expo.*, Sep. 2013, pp. 2239–2244.

[68] M. Hanazawa, N. Sakai, and T. Ohira, "SUPRA: Supply underground power to running automobiles," in *Proc. IEEE Int. Electric Vehicle Conf.*, Greenville, SC, USA, Mar. 2012, pp. 1–4.

[69] S. Y. Choi, B. W. Gu, S. Y. Jeong, and C. T. Rim, "Advances in wireless power transfer systems for roadway-powered electric vehicles," *IEEE J. Emerg. Sel. Topics Power Electron.*, vol. 3, no. 1, pp. 18–36, Mar. 2015.

[70] J. Schneider, "SAE J2954 overview and path forward," Soc. Automot. Eng. Int., Warrendale, PA, USA, 2012.

[71] Guidelines for limiting exposure to time-varying electric and magnetic fields (Up to 300 GHz), ICNIRP Guidelines, 1998.

[72] Guidelines for limiting exposure to time-varying electric and magnetic fields (Up to 100 kHz), ICNIRP Guidelines, 2010.

[73] S. Y. Ahn, J. S. Park, and J. H. Kim, "Low frequency electromagnetic field reduction techniques for the on-line electric vehicles (OLEV)," in *Proc. IEEE Int. Symp. Electromagn. Compat.*, 2010, pp. 625–630.

[74] J. H. Kim and J. H. Kim, "Analysis of EMF noise from the receiving coil topologies for wireless power transfer," in *Proc. Asia-Pacific Symp. Electromagn. Compat.*, 2012, pp. 645–648.

[75] H. S. Kim and J. H. Kim, "Shielded coil structure suppressing leakage magnetic field from 100W-class wireless power transfer system with higher efficiency," in *Proc. IEEE Microw. Workshop Ser. Innovative Wireless Power Transmiss. Technol., Syst. Appl.*, 2012, pp. 83–86.

[76] S. Y. Ahn, H. H. Park, and J. H. Kim, "Reduction of electromagnetic field (EMF) of wireless power transfer system using quadruple coil for laptop applications," in *Proc. IEEE Microw. Workshop Series Innovative Wireless Power Transmiss. Technol., Syst. Appl.*, 2012, pp. 65–68.

[77] S. C. Tang, S. Y. R. Hui, and H. S. Chung, "Evaluation of the shielding effects on printed circuit board transformers using ferrite plates and copper sheets," *IEEE Trans. Power Electron.*, vol. 17, no. 6, pp. 1080–1088, Nov. 2002.

[78] X. Liu and S. Y. R. Hui, "An analysis of a double-layer electromagnetic shield for a universal contactless battery charging platform," in *Proc. IEEE Power Electron. Specialists Conf.*, Jun. 2005, pp. 1767–1772.

[79] P. Wu, F. Bai, Q. Xue, and S. Y. R. Hui, "Use of frequency selective surface for suppressing radio-frequency interference from wireless charging pads," *IEEE Trans. Ind. Electron.*, vol. 61, no. 8, pp. 3969–3977, Aug. 2014.

[80] M. L. Hiles and K. L. Griffing, "Power frequency magnetic field management using a combination of active and passive shielding technology," *IEEE Trans. Power Del.*, vol. 13, no. 1, pp. 171–179, Jan. 1998.

[81] C. Buccella and V. Fuina, "ELF magnetic field mitigation by active shielding," in *Proc. IEEE Int. Symp. Ind. Electron.*, 2002, pp. 994–998.

[82] J. Kim *et al.*, "Coil design and shielding methods for a magnetic resonant wireless power transfer system," *Proc. IEEE*, vol. 101, no. 6, pp. 1332–1342, Jun. 2013.

[83] S. Y. Hoon, B. H. Choi, E. S. Lee, and C. T. Rim, "General unified analyses of two-capacitor inductive power transfer systems: Equivalence of current-source SS and SP compensations," *IEEE Trans. Power Electron.*, vol. 30, no. 11, pp. 6030–6045, Nov. 2015.

[84] V. X. Thai, S. Y. Choi, S. Y. Jeong, and C. T. Rim, "Coreless power supply rails compatible with both stationary and dynamic charging of electric vehicles," in *Proc. IEEE Int. Future Energy Electron. Conf.*, 2015, pp. 1–5.

[85] J. H. Kim, B. S. Lee, J. H. Lee, and J. H. Baek, "Development of 1MW inductive power transfer system for a high speed train," *IEEE Trans. Ind. Electron.*, vol. 62, no. 10, pp. 6242–6250, Oct. 2015.

[86] General Concepts of VICTORIA Project in Endesa Website. (2013). [Online]. Available: http://www.endesa.com/en/saladeprensa/noticias/wireless-en-route-charging-electric-buses

[87] E. Mascarell, "VICTORIA: Towards an intelligent e-mobility," presented at the UNPLUGGED Final Event, 2015.

[88] J. A. Ruiz, "ITS systems developing in Malaga," presented at the 2nd Congr. EU Core Net Cities, 2014.

[89] General Information of INTIS for Developments of Wireless Electric Vehicles in INTIS Website. (2016). [Online]. Available: http://www.intis.de/intis/mobility.html
[90] Technical Article eCarTec of INTIS Website. (2014). Online. [Available]. http://www.intis.de/intis/downloads_e.html
[91] Technical Information 30 kW coil system VW T5 transporter in INTIS Website. (2014). [Online]. Available: http://www.intis.de/intis/downloads_e.html
[92] G. A. Covic and J. T. Boys, "Inductive power transfer" *Proc. IEEE*, vol. 101, no. 6, pp. 1276–1289, Jun. 2013.
[93] K. B. Lee, Z. Pantic, and S. M. Lukic, "Reflexive field containment in dynamic inductive power transfer systems," *IEEE Trans. Power Electron.*, vol. 29, no. 9, pp. 4592–4602, Sep. 2014.
[94] J. Shin *et al.*, "Design and implementation of shaped magnetic-resonance-based wireless power transfer system for roadway-powered moving electric vehicles," *IEEE Trans. Ind. Electron.*, vol. 61, no. 3, pp. 1179–1192, Mar. 2014.
[95] G. A. Covic, J. T. Boys, M. L. Kissin, and H. G. Lu, "A three-phase inductive power transfer system for roadway-powered vehicles," *IEEE Trans. Ind. Electron.*, vol. 54, no. 6, pp. 3370–3378, Dec. 2007.
[96] L. Chen, G. R. Nagendra, J. T. Boys, and G. A. Covic, "Double-coupled systems for IPT roadway applications," *IEEE J. Emerg. Sel. Topics Power Electron.*, vol. 3, no. 1, pp. 37–48, Mar. 2015.
[97] C. B. Park, S. W. Lee, G. H. Choi, and C. T. Rim, "Innovative 5-m-off-distance inductive power transfer systems with optimally shaped dipole coils," *IEEE Trans. Power Electron.*, vol. 30, no. 2, pp. 817–827, Nov. 2014.
[98] C. T. Lim and G. H. Cho, "New approach to analysis of quantum rectifier-inverter," *Electron. Lett.*, vol. 25, no. 25, pp. 1744–1745, Dec. 1989.

Chunting Chris Mi (S'00–A'01–M'01– SM'03–F'12) received the B.S.E.E. and M.S.E.E. degrees in electrical engineering from Northwestern Polytechnical University, Xi'an, China, in 1985 and 1988, respectively, and the Ph.D. degree in electrical engineering from the University of Toronto, Toronto, ON, Canada, in 2001.

He is currently a Professor and the Chair of Electrical and Computer Engineering at San Diego State University, San Diego, CA, USA. He is also the same time, he is an Adjunct Professor of electrical and computer engineering and the Director of the Department of Energy-funded Graduate Automotive Technology Education Center for Electric Drive Transportation, University of Michigan, Ann Arbor, MI, USA. His research interests include electric drives, power electronics, electric machines, renewable-energy systems, and electrical and hybrid vehicles. He has conducted extensive research and has published more than 100 journal papers.

Prof. Mi is an Area Editor of the IEEE Transactions on Vehicular Technology and an Associate Editor of the IEEE Transactions on Power Electronics and IEEE Transactions on Industry Applications.

Giuseppe Buja (M'75–SM'84–F'95-LF'13) received the Laurea (Hons.) degree from the University of Padova, Padova, Italy, in 1975.

He is currently a Full Professor at the University of Padova, heading the laboratory on "Electric Systems for Automation and Automotive." He has carried out research in the field of power and industrial electronics and has authored or coauthored more than 200 papers. His current research interests include wired and wireless charging of electric vehicles, and power conversion systems for renewable energies.

Prof. Buja received the IEEE Industrial Electronics Society (IES) Eugene Mittelmann Achievement Award "in recognition of his outstanding technical contributions to the field of industrial electronics". He is currently an Associate Editor of the IEEE Transactions on Industrial Electronics, a Senior Member of the Administrative Committee of the IES, and a member of a number of international scientific associations and conference committees.

Su Y. Choi (S'13–M'16) received the B.S. degree in mechanical engineering from Pusan National University, Pusan, Korea, and the Integrated Master's and Ph.D. degree in nuclear and quantum engineering from the Korea Advanced Institute of Science and Technology (KAIST), Daejeon, Korea, in 2011 and 2016, respectively.

He is currently developing inductive power transfer systems for roadway powered electric vehicles in the Nuclear Power Electronics and Robots Laboratory (PEARL), KAIST, as a Postdoctoral Researcher. His research interests include power converters, inductive power transfer systems, and power supply systems for mobile robots.

Chun T. Rim (M'90–SM'11) received the B.S. degree (Hons.) from the Kumoh Institute of Technology, Gumi, Korea, in 1985, and the M.S. and Ph.D. degrees from the Korea Advanced Institute of Science and Technology (KAIST), Daejeon, Korea, all in electrical engineering, in 1985, 1987, and 1990, respectively.

Since 2007, he has been an Associate Professor of nuclear and quantum engineering at KAIST. He has authored or coauthored 142 technical papers, written 8 books, and holds 141 patents (awarded and pending).

Dr. Rim received the Best Paper Award of IEEE Transactions on Power Electronics (TPE) in 2015 (wireless power) and three prizes from the Korean government. He is currently an Associate Editor of IEEE TPE and the IEEE Journal of Emerging and Selected Topics in Power Electronics (J-ESTPE), a Guest Editor of the Special Issue on Wireless Power Transfer of the IEEE TPE, IEEE Transactions on Industrial Electronics, and J-ESTPE, and the General Chair of the 2014, 2015, and 2016 IEEE VTC-Workshop on Wireless Power.